

## A Tuning Fork Shaped Differential Dipole Antenna with Floating Reflectors

Rida Gadhafi\*, Dan Cracan, Ademola A. Mustapha, and Mihai Sanduleanu

**Abstract**—In this letter, a tuning fork shaped, differential dipole antenna, with two floating reflectors, is presented. The dipole antenna resonates at 1.22 GHz and has a fractional bandwidth (FBW) of 16.39% and a differential impedance of  $100\ \Omega$ . The proposed antenna is composed of quarter wavelength tuning fork shaped dipole arms in the top layer. To improve robustness, while connecting to the differential circuits, two floating reflectors are used on the bottom layer, beneath the dipole arm. This method helps improving the gain by 7%. A microstrip-to-coplanar strip line (CPS) transition is designed to measure the stand-alone differential antenna. The measured gain and efficiency of the antenna are 2.14 dBi and 84%, respectively, at the resonant frequency. The possible targeted applications are circuits with differential inputs/outputs, like energy harvesting circuits, radio frequency tags, wireless communications and any other wireless sensor network nodes. Details of the design along with simulated and experimental results are presented and discussed.

### 1. INTRODUCTION

Differential antennas have a significant role in modern wireless communication world, as they can be easily attached to differential RF circuits. This is achieved without a balun [1, 2]. They can be designed together with differential Low Noise Amplifiers (LNAs) or Power Amplifiers (PAs) allowing the elimination of losses introduced by baluns and matching circuits. The inputs or outputs of differential RF circuits generally have  $50\ \Omega$  terminations, to either ground or the voltage supply, resulting in a  $100\ \Omega$  differential mode impedance. Therefore, the differential impedance of  $100\ \Omega$  for the antenna matches with differential integrated circuits. Microstrip antennas, dipole antennas and loop antennas are commonly used structures in a differential configuration [3–11]. Even though microstrip antennas have smaller sizes and higher gain than dipole antennas, the bandwidth for those antennas is limited. Therefore, they are not the first choice for wideband communications applications [12]. In this scenario, dipole antennas, exhibiting wideband characteristics, render them a good candidate for broadband communications, where differential inputs and/or outputs are needed [1]. However, as the dipole antennas do not possess a ground plane and due to the single layer structure of the dipole, they can be detuned by metallic structures from proximity. This problem can be solved by using a differential design with high Common-Mode Rejection Ratio. For improved performance, existing literature introduces complex structures, like stacked designs or stub designs, making them impractical for consumer type applications [13, 14]. Moreover, even though dipoles are differential in nature, differential characteristics are not well studied, and most of the configurations are single ended with a built in balun for single ended characterization.

In this letter, a tuning fork-shaped, differentially fed, dipole antenna is proposed. For improving robustness, two floating reflectors are placed beneath each dipole arm. By this, the impedance of the antenna is not changed when connecting to differential loads. This method helped to improve the gain

---

*Received 9 October 2018, Accepted 12 November 2018, Scheduled 23 November 2018*

\* Corresponding author: Rida Gadhafi (rida.gadhafi@ku.ac.ae).

The authors are with the Khalifa University of Science and Technology, Abu Dhabi 54224, United Arab Emirates.

by 7%. The tuning fork dipole arm is approximated as a quarter wavelength size. The antenna ensures a differential impedance of  $100\ \Omega$  and has an impedance bandwidth of 16.39%. To enable differential feed, an L-shaped coplanar strip line, optimized for  $50\ \Omega$  in single ended mode, is placed at each arm. Furthermore, for characterizing the stand-alone antenna, a microstrip-to-coplanar strip transition is designed at the input. The simulated and measured results of the antenna are compared. Section 2 describes the antenna design. Section 3 presents the simulated and measured results and discusses the discrepancies between the two followed by Conclusions in Section 4.

## 2. ANTENNA DESIGN

The structure of the proposed, tuning fork shaped, differential-fed, dipole antenna is shown in Fig. 1. The substrate used for antenna fabrication is low cost FR-4 with dielectric permittivity of 4.4 and tangent loss of 0.025. The substrate has a thickness of 1.6 mm. As shown in Fig. 1, the antenna is composed of two symmetrical tuning-fork shaped arms, positioned at a gap  $g$  and fed by  $100\ \Omega$ , L-shaped, coplanar strip line. CPS was optimized to present an input impedance of  $100\ \Omega$  in the differential mode (equivalent to  $50\ \Omega$  in single ended mode). The width of the two symmetric strips was chosen to be 3 mm, and the gap between them was 0.2 mm. The L-shaped feed line is extended from the center of the arm such that the resonating arms will be less influenced by the external circuits.

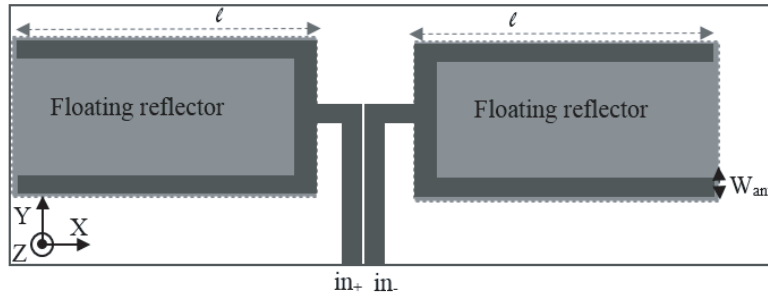


**Figure 1.** Geometry of the antenna. The top copper layer is indicated in dark gray. The bottom copper layer is indicated in light gray. ( $l = 36\ \text{mm}$ ,  $W_{ant} = 2\ \text{mm}$ ;  $\epsilon_r = 4.4$ ,  $\tan \delta = 0.015$ , and  $h = 1.6\ \text{mm}$ ).

The dipole arm constitutes a tuning fork shaped structure. The length  $l$  of the arm is approximated as a quarter guided wavelength, by using the standard formula:

$$l = \frac{c}{4f_c \sqrt{\epsilon_{reff}}} \quad (1)$$

where  $\epsilon_{reff}$ ,  $c$ , and  $f_c$  are, respectively, the effective dielectric permittivity, the velocity of light in free space, and the resonant frequency of the antenna, respectively. Two floating reflectors are placed beneath each dipole arm. The challenge was to keep the same impedance of the antenna and improving its robustness while connecting to the associated circuits, in a differential mode. The partial floating metal can act as a reflector which allows the energy to radiate efficiently to free space by preventing the lossy FR-4 substrate to absorb the power. This, in turn, increases the gain by 7%.

The intrinsic antenna has a dimension of  $9\ \text{cm} \times 1.8\ \text{cm}$ . In order to characterize the stand-alone antenna, two microstrip feeding lines were added, as shown in Fig. 2. This allows the connection of the antenna to a vector network analyzer by means of standard SMA connectors. The width of the dipole arm is optimized to obtain impedance matching at the operating frequency, and the width of the microstrip line is optimized for  $50\ \Omega$  characteristic impedance. Parametric simulations were carried out to choose the optimum value.

Figures 3(a) and (b) show the change in real and imaginary parts of the differential impedance for different arm widths ( $W_{ant}$ ). At resonant frequency, the real and imaginary parts of the differential impedance are  $100\ \Omega$  and  $10\ \Omega$ , respectively. This inductive effect could be explained by the presence of extended feed line. At the same time, the imaginary part changes from inductive to capacitive in the

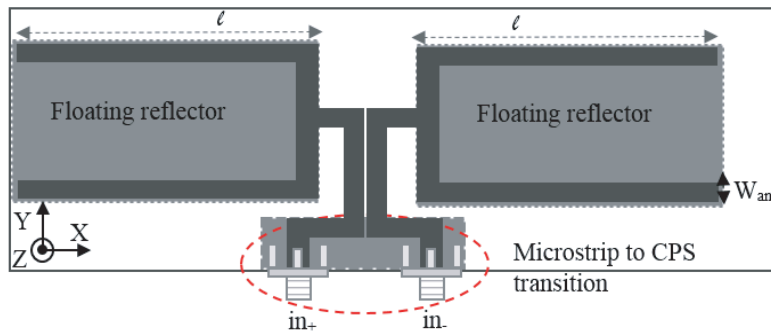


**Figure 2.** Layout of the standalone differential antenna with microstrip to coplanar strip line transition. The top copper layer is indicated in dark gray. The bottom copper layer is indicated in light gray.

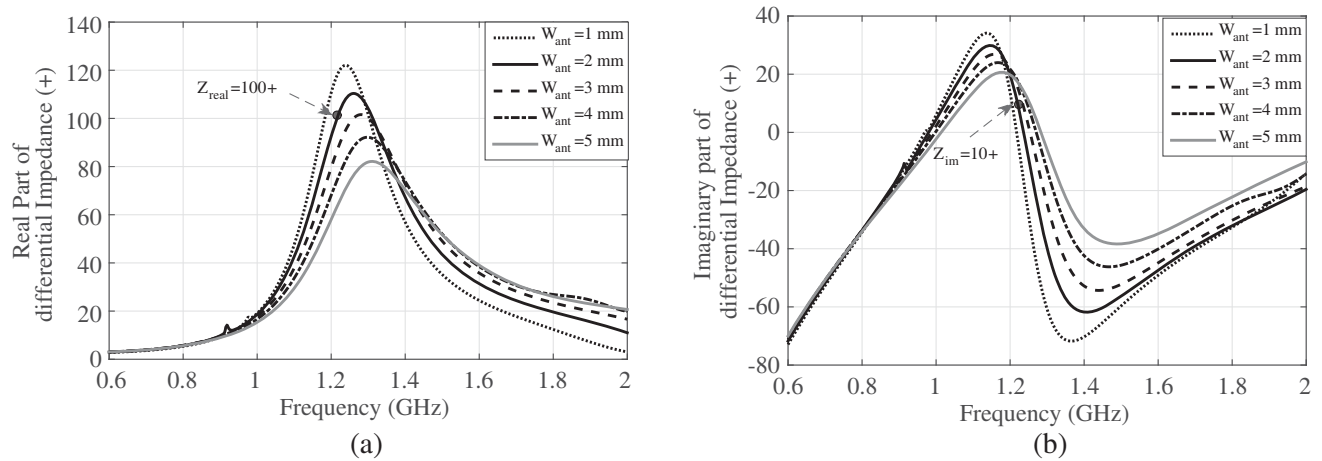


**Figure 3.** The (a) real and (b) imaginary parts of the differential impedance of the antenna for different arm widths  $W_{ant}$ . Dark line shows the proposed antenna.

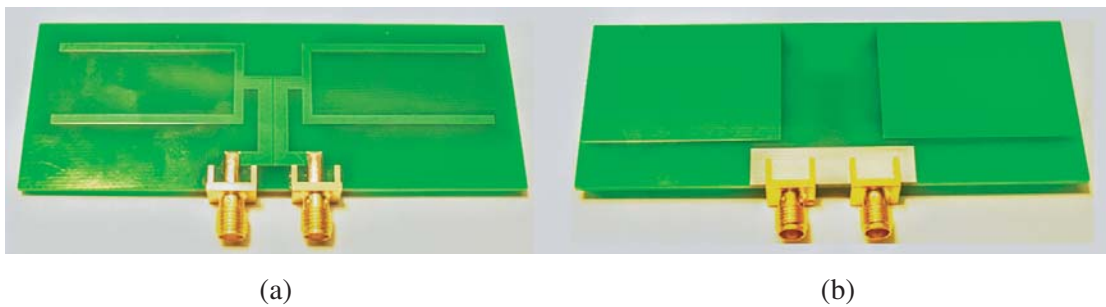


**Figure 4.** Differential antenna. (a) Front view, (b) back view.

frequency band of 1.1 GHz to 1.3 GHz. Fig. 4 shows the fabricated stand-alone antenna. The fabricated antenna has a dimension of 9 cm × 2.3 cm including the feedline.

### 3. MEASUREMENT RESULTS AND DISCUSSION

This section describes the simulated and measured results of the proposed antenna. The antenna was simulated using Ansys HFSS, and measurements were conducted using Agilent Network Analyzer

(PNA-X N5242A). A commercially available balun from Marki Microwave [15] is used to drive the differential-fed dipole antenna. The input of the balun was connected to one port of the network analyzer, and the two output ports were connected to the two inputs of the antenna. The differential  $S$ -parameters were measured. Fig. 5 shows the simulated and measured input return losses ( $S_{11}$ ) of the antenna. The losses in the measured curve are attributed to the balun. Balun introduced frequency dependent losses as explained in the datasheet [15].

The radiation characteristics of the antenna are measured inside an anechoic chamber. A standard horn antenna, a network analyzer and MATLAB controlled turn-table were used in the measurement setup. To perform the far-field measurements, the horn antenna and the antenna under test were separated at a distance of 1.5 m. The comparison of simulated and measured radiation patterns of the

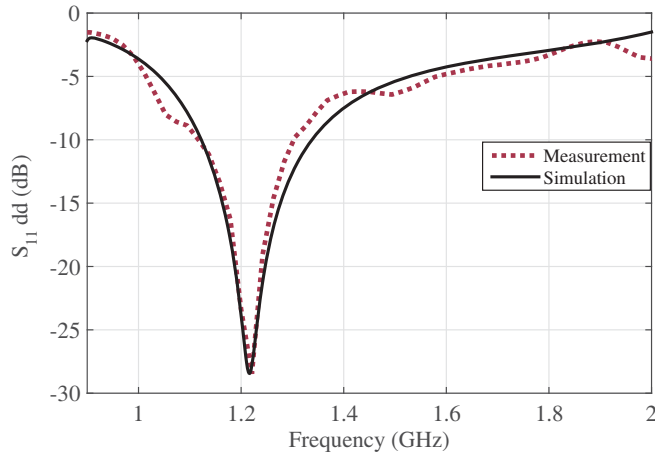


**Figure 5.** Return loss characteristics of the proposed antenna ( $l = 36$  mm,  $W_{ant} = 2$  mm,  $\epsilon_r = 4.4$ ,  $\tan \delta = 0.015$ , and  $h = 1.6$  mm).

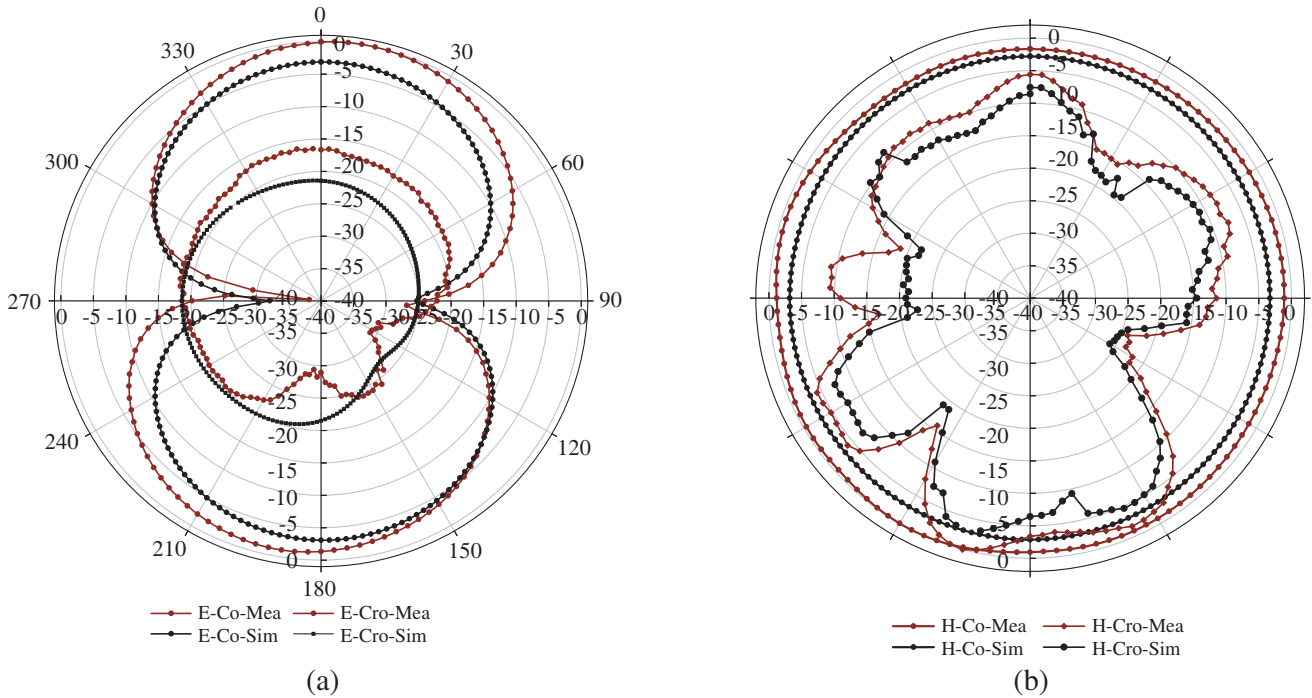


**Figure 6.** Simulated and measured radiation patterns of the proposed antenna at 1.22 GHz. (a)  $E$ -plane, (b)  $H$ -plane.

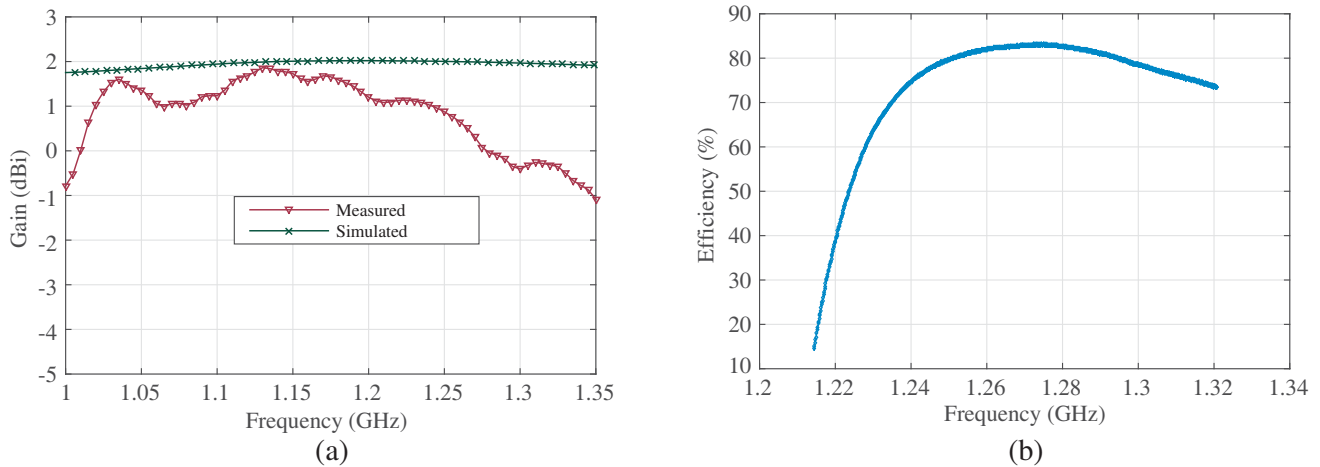


**Figure 7.** Gain and efficiency of the dipole antenna. (a) Simulated and measured gain of the dipole antenna, (b) measured efficiency of the dipole antenna.

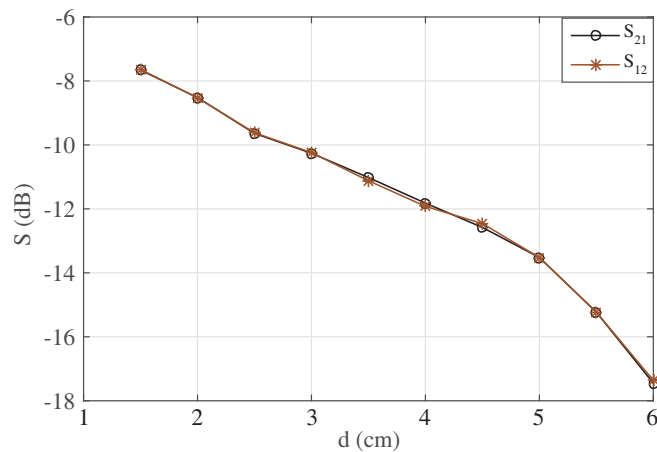


**Figure 8.** Power transfer curve of the proposed antenna as a function of distance  $d$ .

antenna at the resonant frequency are shown in Figs. 6(a) and (b). The passive components (coaxial cables and balun) used for the measurement introduced small losses, as seen in the measured curve. As seen in the figure, the antenna exhibits figure of eight radiation patterns in the  $y$ - $z$  plane. In the  $x$ - $z$  plane, the pattern is more omnidirectional. The co-polar and cross-polar isolations in the horizontal plane ( $E$ -plane or  $y$ - $z$  plane) are in the order of 18 dB and around 5 dB in the vertical plane ( $H$ -plane or  $x$ - $z$  plane). Fig. 7(a) shows the comparison between simulated and measured gains. As shown, the antenna has a simulated gain of 2.14 dBi and measured gain of 1.9 dBi at the center frequency. Due to losses from the external balun, measured gain exhibits more nonuniform nature throughout the bandwidth than the simulated one, where the gain is uniform. When connecting the antenna directly to the circuit, the losses will be eliminated. The measured efficiency of the antenna is 84%, as shown in Fig. 7(b). The antenna also shows an impedance bandwidth of 200 MHz at 1.22 GHz band, from 1.1 GHz to 1.3 GHz.

The power transfer capability of the differential antenna was tested as discussed in [16]. Two identical differential dipole antennas were placed face-to-face, separated at a distance  $d$ . The two ports of the network analyzer were connected to the input ports of each balun. Power transmitted/received at each port as a function of distance was measured and plotted as shown in Fig. 8. Distance  $d$  was chosen in a range of 1.5 cm to 6 cm. The measurement was conducted in lab environment and not in an anechoic chamber.

#### 4. CONCLUSIONS

A tuning fork-shaped differential dipole antenna, operating at 1.22 GHz, is presented. For improving robustness, two floating reflectors are placed beneath each dipole arm. By this, the impedance of the antenna is not changed when connecting to differential loads. This method helps to improve the gain by 7%. The dipole arm is approximated as a quarter wavelength. The antenna has a differential impedance of  $100\ \Omega$ . By this, the antenna could be directly connected to a balanced integrated circuit input/output. Experimental results show that the antenna has impedance bandwidth of 16.39%. It also exhibits a measured gain of 1.9 dBi and measured efficiency of 84%. There are many applications for the differential antenna. To enumerate a few, the antenna finds its application in energy harvesting circuits, RF tags and any wireless sensor network nodes where differential inputs/outputs are needed.

#### REFERENCES

1. Ding, C. and K. M. Luk, "Compact differential fed dipole antenna with wide bandwidth stable gain and low cross polarization," *Electronic Letters*, Vol. 53, No. 15, 1019–1021, 2017.
2. Xue, Q., X. Zhang, and C. H. Chin, "A novel differential fed patch antenna," *IEEE Antennas Wirel. Propag. Lett.*, Vol. 5, No. 1, 471–474, 2006.
3. Scorcioni, S., L. Larcher, and A. Bertacchini, "A reconfigurable differential CMOS RF energy scavenger with 60% peak efficiency and 21 dBm sensitivity," *IEEE Microw. Wireless Compon. Lett.*, Vol. 23, No. 3, 155–157, 2013.
4. Powell, J. and A. Chandrakasan, "Differential and single ended elliptical antennas for 3.1–10.6 GHz ultra-wideband communication," *IEEE Antennas Propag. Symposium*, Vol. 3, 2935–2938, 2004.
5. Schantz, H., "Planar elliptical element ultra-wideband dipole antennas," *IEEE Antennas Propag. Symposium*, Vol. 3, 44, 2002.
6. Liu, N. W., L. Zhu, W. W. Choi, and J. D. Zhang, "A differential fed microstrip patch antenna with bandwidth enhancement under operation of TM<sub>10</sub> and TM<sub>30</sub> modes," *IEEE Trans. Antennas Propag.*, Vol. 65, No. 4, 1607–1614, 2007.
7. Zhang, H. and H. Xin, "A dual band dipole antenna with integrated balun," *IEEE Trans. Antennas Propag.*, Vol. 57, No. 3, 786–789, 2009.
8. Pepe, D., L. Vallozi, H. Rogier, and D. Zito, "Planar differential antenna for short range UWB pulse radar sensor," *IEEE Antennas Wirel. Propag. Lett.*, Vol. 12, 1527–1530, 2013.
9. Liu, N. W., L. Zhu, W. W. Choi, and J. D. Zhang, "A novel differential fed patch antenna on stepped impedance resonator with enhanced bandwidth under dual resonance," *IEEE Trans. Antennas Propag.*, Vol. 64, No. 11, 4618–4625, 2016.
10. Tang, Z., J. Liu, and Y. Yin, "Enhanced cross polarization discrimination of wideband differentially fed dual polarized antenna via a shorting loop," *IEEE Antennas Wirel. Propag. Lett.*, Vol. 17, No. 8, 1454–1458, 2018.
11. Le, T., K. Mayaram, and T. Fiez, "Efficient far field energy harvesting for passively powered sensor networks," *IEEE J. Solid-State Circuits*, Vol. 43, No. 5, 1287–1302, 2008.
12. Arrawatia, M., M. S. Bhaghni, and G. Kumar, "Differential microstrip antenna for energy harvesting," *IEEE Trans. Antennas Propag.*, Vol. 63, No. 4, 1581–1588, 2015.
13. Liu, Y. Y. and Z. H. Tu, "Differential enhanced broadband dual polarized printed dipole antenna for base stations," *Microwave and Opt. Tech. Letters*, Vol. 58, No. 12, 2864–2868, 2016.
14. Xie, J.-J. and Q. Song, "Wideband dual-polarized dipole antenna with differential feeds," *Progress In Electromagnetics Research Letters*, Vol. 59, 43–49, 2016.
15. Electrical Specifications Data Sheet, [online], available at [www.markimicrowave.com](http://www.markimicrowave.com).
16. Gadhafi, R. and M. Sanduleanu, "A modified Patch Antenna with square-open loop resonator slot for improved bandwidth performance for in WiFi applications," *Adv. in Science, Tech. and Engineering Systems J.*, Vol. 2, No. 3, 1467–1471, 2017.